Low-cost irradiance sensors for irradiation assessments inside tree canopies

M.A. Muñoz-García , A. Melado-Herreros , J.L. Balenzategui , P. Barrerio

Abstract

The solar irradiation that a crop receives is directly related to the physical and biological processes that affect the crop. However, the assessment of solar irradiation poses certain problems when it must be measured through fruit inside the canopy of a tree. In such cases, it is necessary to check many test points, which usually requires an expensive data acquisition system. The use of conventional irradiance sensors increases the cost of the experiment, making them unsuitable. Nevertheless, it is still possible to perform a precise irradiance test with a reduced price by using low-cost sensors based on the photovoltaic effect.

The aim of this work is to develop a low-cost sensor that permits the measurement of the irradiance inside the tree canopy. Two different technologies of solar cells were analyzed for their use in the measurement of solar irradiation levels inside tree canopies. Two data acquisition system setups were also tested and compared. Experiments were performed in Ademuz (Valencia, Spain) in September 2011 and September 2012 to check the validity of low-cost sensors based on solar cells and their associated data acquisition systems. The observed difference between solar irradiation at high and low positions was of $18.5\% \pm 2.58\%$ at a 95% confidence interval.

Large differences were observed between the operations of the two tested sensors. In the case of a-Si cells based mini-modules, an effect of partial shadowing was detected due to the larger size of the devices, the use of individual c-Si cells is recommended over a-Si cells based mini-modules.

1. Introduction

There are different methods and experimental procedures used to determine the amount of solar irradiance at a given point. The conventional, accurate assessment of solar radiation in many engineering and scientific applications at a ground level is usually based on thermopile-type devices (pyranometers, pyrheliometers). However, these are quite expensive sensors for the purpose of this research. The objective of this work is to evaluate the effectiveness of a means for the detection of solar irradiation using a more cost-effective irradiance sensor with an acceptable error ($\pm 5\%$), adequate for applications where a relative evaluation of irradiance in a distributed area is of high importance.

The sun supplies energy by means of solar radiation over time (irradiation). The solar radiation intensity (irradiance) normal to the direct beam radiation from the sun outside the atmosphere at the mean earth–sun distance

is called the solar constant. The solar constant has been estimated to be 1370 W/m^2 with a spectral distribution from 200 nm to beyond 4000 nm and beyond (one of the models is known as ASTM E-490. Nevertheless, the atmosphere absorbs some parts of the spectrum, as most UV radiation does, and not all the radiation reaches the Earth's surface. According to IEC 60904-3, the radiation that reaches the surface ranges from 300 nm to 4095 nm. The maximum for the irradiance and the average irradiation also change depending on the region. In the south of Europe, around 1000 W/m^2 reaches the ground at midday on sunny days in the spring and fall. The accumulated irradiance is known as irradiation and can be measured in W h/m^2 or J/m^2. The global radiation is composed of two components: direct or beam radiation (straight rays from the sun) and indirect or diffuse radiation. The spectral distribution of both components is not the same. According to some previous studies focused on the effect of the radiation diffusion due to tree crop, the indirect radiation makes up a greater portion of UV radiation(Parisi et al., 2000).

The solar radiation can also be estimated through combining satellite images with solar radiation data available from a grid of recording stations around the world, which is also based on pyranometers, and specific algorithms for the calculation of daily irradiation (Zarzalejo et al., 2009). With this technique, the local air temperature data can be also used to determine the evapotranspiration (E0) of a crop (Bois et al., 2008). Additionally, neural networks can be used for the estimation of the net radiation without the use of a net of pyranometers sensors (Geraldo-Ferreira et al., 2011). These instruments are not among the most expensive compared to those that are focused on measuring the solar spectrum (Eltbaakh et al., 2011). It is not possible to determine the radiation inside a crop with these methods.

Another available option for estimating solar radiation is the use of calibrated photodetectors (photodiodes, solar cells) protected inside a case, in some cases with some electronic circuitry to adapt output signals to recording instrumentation [Glotzbach, Zehner] or even to ensure the short circuit condition in the case of solar cells (Plesz et al., 2011). For example, in many photovoltaic plants, the irradiance is evaluated by means of so-called "equivalent technology solar cells" (Martin and Ruiz, 2001), a large area photovoltaic solar cell with the same characteristics of those used to produce energy.

The analysis of the solar radiation that a crop receives supplies valuable information. In some cases, solar radiation is related to physiological disorders such as watercore (Melado-Herreros et al., 2012). Radiation is not homogeneous throughout the plant, as the shade of the upper parts affect the lower parts. In the case of crops like grape vines, previous studies have estimated the solar radiation using the measured temperature. The solar radiation (short wave radiation) can be related to thermal radiation (long wave radiation) (Pieri, 2010). In this case, the model was obtained for net solar radiation in different parts of the crop but not at different height levels of the canopy. Nevertheless, the model obtained the net radiation that reached the crop, compared to the part that reached the soil.

Some previous studies have focused on the detection of solar radiation inside and under the canopy of trees. Some of them used photodiodes and optical filters for the detection of photosynthetically active radiation (PAR) (Palva et al., 2001), and others based the sensor on a thermocouple (Abraha and Savage, 2010). Both analyzes obtained a three-dimensional model for the interception of the radiation by the tree crops.

Studies dealing with the influence of trees over scattered radiation, in terms of the solar spectrum, have also been carried out (Heisler et al., 2003). In Heisler's study, the research was focused on the percentages of PAR, UV, and IR present in the radiation that reached the space under different types of trees such as red oak (*Quercus rubra*), red maple (*Acer rubrum*), white ash (*Fraxinus americana*), ginkgo (*Ginkgo biloba*), and thornless (*Liquidambar styraciflua*). The conclusion was that the relative irradiance Ir (irradiance beneath trees/above-canopy irradiance) strongly depended on the position and the wavelength. For the PAR radiation in leaves, the Ir ranged from 16% in the shade to 97% in the sunlight.

Another experiment determined the radiation interception by olive canopies (Mariscal et al., 2000). This is another case where PAR radiation sensors based on thermopile (LI-CORE) were used. The effect of the leaves was evaluated, and their shapes were taken into account to determine a model that could explain the radiation intercepted by the tree. A transmittance model for PAR radiation was achieved. It was found that the transmittance of the olive leaves was below 1% and the reflectance ranged from 6% to 12%, depending on the part of the leaf. This data allows for the estimation of the radiation interception for this type of tree.

Although these studies provided good results, they used expensive sensors for the detection of radiation in different bandwidths. An alternative to these high cost sensors is the use of commercially available small solar cells. In this sense, the semiconductor making the solar cell will determine an approximation for the spectrum of the radiation detected. While using a crystalline silicon cell the irradiance detected will cover about 80% of the solar spectral distribution, using an amorphous silicon a-Si:H cell that will have a narrower spectral response (about a 65% of the solar spectrum). The use of different technologies can also give information not only about the quantity of radiation that reaches the crop but also about the kind of radiation. This is very important for crops as it is directly related to Photo-Active Radiation.

2. Objectives

This study had two objectives. The first was to examine different photovoltaic sensors in order to obtain a more cost-effective system for measuring solar radiation inside

tree canopies. Sensors of two different photovoltaic technologies and with different configurations were evaluated.

The second objective of this study was to two acquisition systems: a PC that was powered by a photovoltaic system and a traditional data logger powered by a sole battery.

Additionally, the radiation data obtained inside the canopy of an apple tree orchard and the analysis of the relationship between the solar radiation and the physiological disorder known as watercore is examined in a parallel work (Melado-Herreros et al., 2012). Finally, the authors discuss the advantages and disadvantages of each technology for the radiation data logging in field experiments.

3. Materials and methods

The present study was carried out over two years (2011 and 2012) in a commercial apple trees orchard (variety, Esperiega) located in Ademuz (Valencia, Spain), GPS coordinates: 40°4′ 42,13″N, 1°15′ 51,56″W. Each year, the experiment lasted approximately four weeks during September and October, coinciding with the apples' ripening period. The test dates were 16/9 to 11/10 (26 days) in 2011 and 12/9 to 8/10 (27 days) in 2012.

We must take into account that the shape of the trees determined maximum sunlight entry in the lower parts of the trees. To increase sunlight entry, the trees were pruned to orient the tree axis east to west.

The sensors used were based on solar cells in both cases. Before the calibration of the solar cells as solar radiation sensors, a pre-conditioning period was necessary to expose the solar cells to sunlight for some days or weeks. This step is mandatory for a-Si cells and of a high importance for c-Si cells. During the pre-conditioning period, the solar cells achieved their final electrical characteristics. This means that the electrical characteristics of the cell (short circuit current, open circuit voltage, and maximum power) achieved the stable state after a decrease in their value in the initial weeks of exposure to sunlight.

The calibration process consisted of exposing cells with the same orientation to the sun to solar radiation during several clear sunny days and comparing their short circuit current with the radiation given by a reference based on a laboratory calibrated cell, model Si-02-K manufactured by Ingenieurbüro. The accuracy of this reference cell was tested in CIEMAT using a pyranometer: Kipp & Zonen, model CM21.

In order to obtain the short circuit current of the cells to be calibrated, a precision shunt resistor of 1 Ω/1% was used. The measurements were recorded by the same data logger used in the field and described later.

The results of the calibration process are offered in Tables 1 and 2.

3.1. The use of solar cells for irradiation assessment

A solar cell is a device based on the union of two types of semiconductors that form a potential barrier. In such a structure, solar irradiance could extract electrons of the semiconductor. The extracted electrons would be guided outside the device pushed by the potential difference. This phenomenon is known as the photovoltaic effect, and it is possible to obtain an electrical current related to the irradiance received by the device. Solar irradiance is related to the current generated by a cell according to the following formula included in IEC-60891:

$$Isc = I_R sc \frac{G}{G_R}[1 + \alpha(T - T_R)] \quad (A) \tag{1}$$

where Isc is the measured short circuit current, $I_R sc$ is the short circuit current at standard test conditions (an irradiance of $G_R = 1000\ W/m^2$ and a cell temperature of $T_R = 25\ °C$), G is the irradiance, α is the normalized temperature coefficient, and T is the cell temperature.

Nevertheless, for the purposes of this work, and within the global margin of error assumed admissible for a comparative analysis of irradiance at different locations inside the canopy, α is insignificant and not taken into account, especially in the case of a-Si:H devices, as is later discussed. The simplified formula would be:

$$Isc = I_R sc \frac{G}{G_R} \quad (A) \tag{2}$$

Temperature coefficients for short-circuit current are usually low for amorphous silicon devices (+0.08%/K for the used device: AM-5608), and a bit larger for crystalline silicon cells (+0.29%/K for the used device: KXOB22). A 15 K span in the working temperature of the cell along the sunny period of the day would represent differences of about ±0.6% in measured irradiance values for amorphous silicon devices (±2.2% for c-Si cells) between maximum and minimum recorded values. These differences are partially mitigated because the calibration constant of every cell is calculated with the same procedure, using the same recording instrument, in the same period of the year (similar temperature span and max/min values). And to consider the error introduced already accounted for in the global uncertainty budget (±5% in irradiance) for this kind of experiment, in which relative (more than absolute) differences in irradiance are of importance.

A more accurate testing methodology would require the measurement of the individual temperature of every particular cell in order to calculate a temperature-corrected I current and then, a more accurate irradiance evaluation for every point. However, this would reduce the amount of testing points for irradiance to a half of the available channels and would increase the cost of the whole system.

Solar irradiation is the sum of the irradiance during a period of time. In the present work, we obtained the solar irradiation by measuring the average mean irradiance every one or two minutes (depending on the year) and multiplying it by the elapsed time. As the irradiance is obtained in W/m^2 and the time is counted in hours, we obtained the energy (solar irradiation) in $W\,h/m^2$. This unit corresponds to $3600\ J/m^2$.

Table 1
Radiation constant for a-Si sensors, according to the calibration performed in 2011.

Sensor number	#1	#2	#3	#4	#5	#6	#7	#8	#9	#10	#11	#12	#13	#14
Isc^* (mA)	37.2	37	34.3	40.1	36.8	38.3	37.4	37.7	36.5	38.9	39	35.4	37.5	34.4

Table 2
Radiation constant for c-Si sensors, according to the calibration performed in 2012.

Sensor number	#1	#2	#3	#4	#5	#6	#7	#8	#9	#10	#11	#12	#13	#14	#15	#16
Isc^* (mA)	42.8	42.3	42.6	43.1	43.9	42.8	42.9	43.2	42.5	42.8	42.7	42.5	42.6	42.6	42.4	42.8

The spectrum of solar irradiance is related to the emission of a black body (Gueymard, 2004) but it is not exactly the same, as the atmospheres of the Sun and the Earth absorb part of the irradiance. The spectral response of the solar cell is also related to the obtained current. It is represented in the following equation:

$$R \propto \int I_{SC}\,dt = G(\lambda)S(\lambda)\,d\lambda dt \quad (J/m^2) \tag{3}$$

The formula for cumulative daily irradiation (R) is represented in (3), where G is the irradiance depending on the wavelength (λ), and S is the spectral response of the different solar cell technologies. In our experiment, such spectral response was considered constant for each technology and included during the calibration phase. The measured cumulative irradiation was thus related to the sum of the short circuit current of the cell.

The sunlight's angle of irradiance causes different responses in different technologies and types of encapsulation. This effect was analyzed in previous works (Balenzategui and Chenlo, 2005). In the case of the different types of solar cells used in this work, the influence of the sunlight angle of incidence was not found to be significant.

3.2. Data acquisition systems

Two different acquisition systems were evaluated. In the first year, the system included a battery-powered notebook (Fig. 1) that was charged with a photovoltaic (PV) module. The solar irradiance sensors, based on tiny Sanyo modules, were made of amorphous silicon (a-S). They were connected to two model SB-1608FS data acquisition boards (DAQB) manufactured by Measurements and Computing. Each DAQB comprised eight single-ended channels of 14 bits of conversion. The estimated accuracy for every channel was ±2%. The DAQBs were controlled from the notebook by a program developed with LabVIEW®. The power consumption for the PC-based system was around 20 W, and the daily energy consumption was around 480 W h. The whole system was powered by a 100 Ah lead acid battery charged by a crystalline 150 Wp PV module. With this setup, the daily energy generated around 900 W h. The power source was over dimensioned, but it was very important to ensure the system would operate correctly even over several cloudy days.

During the second year, the data was acquired using a data logger manufactured by Delta Ohm (Fig. 2) in order to compare it to the system that was used the previous year. The solar irradiance sensors based on c-Si cells were connected to the data inputs of the data logger. The device had two ports, each formed by eight single-ended channels. Each channel used 16 bits in the conversion from analog to digital. The estimated accuracy for each channel was ±2%. The data logger was powered by a lead–acid battery, which was also used in the first year (100 Ah). The capacity of the battery was checked in the laboratory before the test in order to ensure it stored enough energy to supply electricity during the entire test.

Both years, the data acquisition systems were used to measure solar radiation above and inside the apple tree canopy and to study the relationship between the irradiation incidence and watercore development (Melado-Herreros et al., 2013).

The energy consumption of the data logger-based system was significantly lower (100 mA at 12 V, which is around 14.4 W h/day or 432 W h/month). This allowed the use of a standalone battery of 12 V and 100 Ah, which supplied at least 600 W h (50% of the total capacity). The data logger system was more efficient than the PC-based system and did not require a PV module.

3.3. Amorphous silicon solar mini-modules

During the first year (2011), a-Si cell based mini-modules and model AM-5608 manufactured by SANYO were used. Each mini-module was formed by six cells connected in series, with an active area of 322.9 mm^2 (8.3 mm × 38.9 mm). The parameters of the mini-modules, according to the manufacturer datasheet, are presented in Table 3.

The effects of power stabilization and light soaking of a-Si cells is well-known (Staebler). In order to achieve the stabilized state of the sensors, a previous experiment of degradation was performed in LPF-TAGRALIA facilities (Fig. 3). The experiment consisted of monitoring the short circuit current (Isc) of the sensors during a two month period (July and August of 2011) to determine when the Isc of

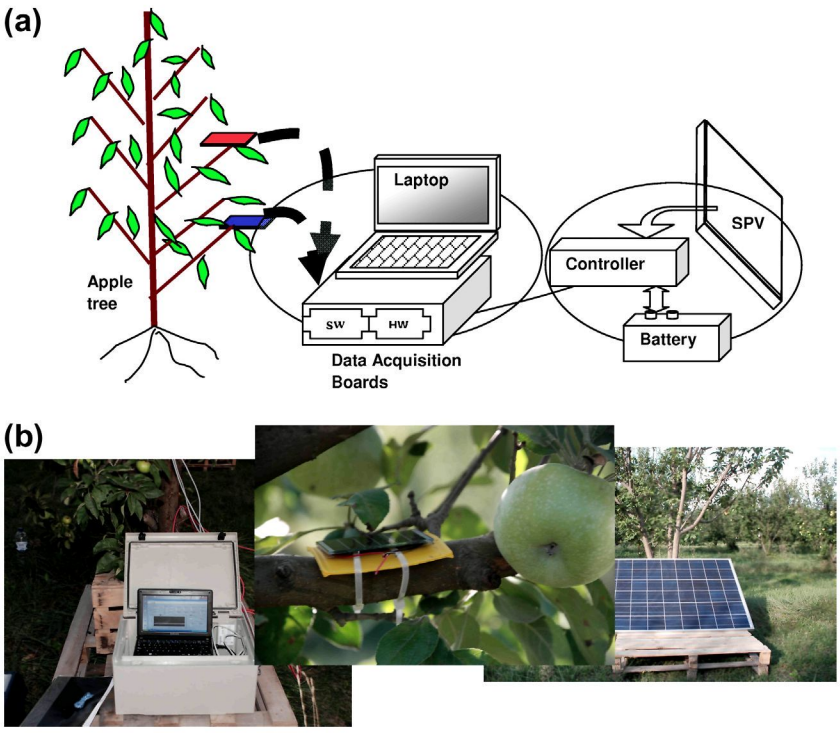

Fig. 1. (a) The setup of the PC based data acquisition system. (b) Some views of the real system.

the sensors stabilize. At the same time within this experiment, Calibration constants were achieved for every sensor.

In total, 14 sensors were installed to monitor the radiation in six trees at two different height levels: 1.5 m and 3 m, corresponding to the bottom and the top of the tree canopy, respectively. Two of the sensors acted as references and were situated over the top of the tree canopy at the end of a support. In total, irradiation data was acquired every two minutes for 26 days.

3.4. Crystalline silicone solar cells

In the second year (2012), a c-Si cell model KXOB22-12X1 manufactured by IXOLAR™ was used. According to the manufacturer datasheet, the nominal short circuit current was around 50 mA. The rest of the electrical characteristics are specified in Table 4. The size of the encapsulated cells is $154\,mm^2$ ($22\,mm \times 7\,mm$). The most significant difference with reference to the previous sensors was that this model includes only a single sensing device instead of several series-connected cells.

In this case, 16 sensors were installed to monitor the radiation in seven trees. Again, two different height levels were used: 1.5 m and 3 m high. As in the previous test, another two sensors acted as reference and were situated above the trees at the end of a support. In total, 18 sensors were used.

Despite the stabilization effect not being very strong in the case of c-Si technology, a small decrease in short circuit current also appeared. It was considered advisable to expose the cells to sunlight for a week. The cell calibration process was sufficient to ensure that the stabilization state was reached. The results of the calibration process determined that the real current, compared to the nominal value (see Table 2), was around 45 mA after two weeks of sunlight exposure.

In this case, the data was recorded using a data logger powered by a stand-alone lead-acid battery, without a PV module. In total, irradiation data was recorded for 27 days in September and October of 2012.

3.5. Statistical analysis

The obtained data were analyzed using a descriptive analysis. For both years of the experiment (Autumn of 2011 and 2012), the following steps were performed with the objective of determining if differences existed between positions:

(a) First, the daily mean of the data for every sensor was calculated and displayed on a dispersion graph, including the high and low positions inside the canopy and the global radiation above the tree.
(b) In the second stage, the mean and the variance of the mean of the measurements were obtained for sensors inside the tree canopy at high and low positions. In this manner, the mean data for the different sensor heights could be compared day by day.
(c) The third stage was a comparison of the mean data at high and low positions within each tree in order to determine if there were anomalous cases in the experiments.

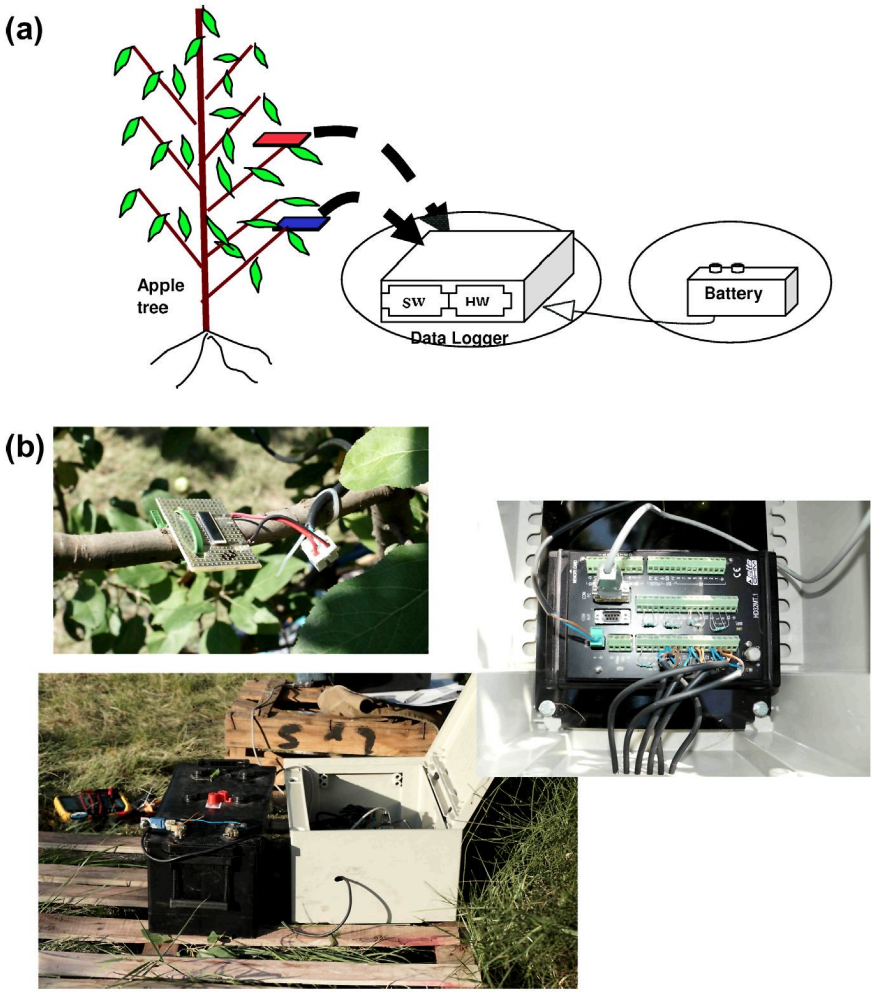

Fig. 2. (a) The setup of the data logger based data acquisition system. (b) Some views of the real system.

Table 3
Manufacturer datasheet of the a-Si sensor used in 2011 tests.

Parameter	Symbol	Test conditions	Results	Units
Open circuit voltage	Voc	50 lux, SS	5.1	V
Short circuit current	*Isc*	50 lux, SS	17.8	mA
Maximum power	Pm	50 lux, SS	59 (Vm 3.9 V; Imp 15.1 mA)	mW
Maximum power	Pm	STC: AM-1.5 100 mW/cm2	125 (Vm 3.9 V; Imp 32 mA)	mW

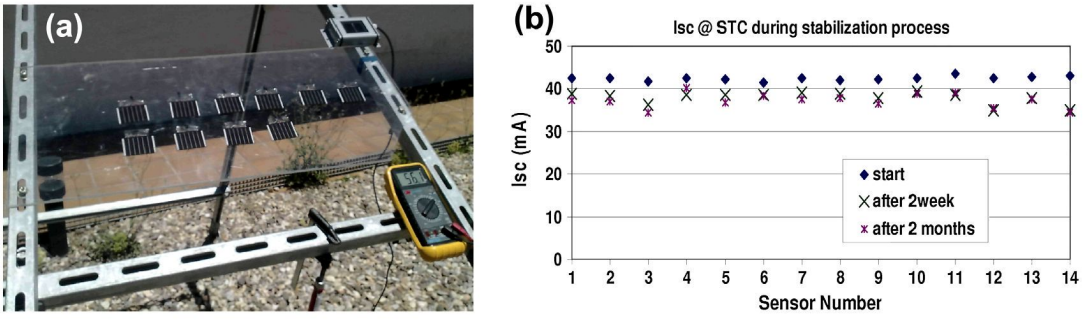

Fig. 3. (a) Setup for the stabilization of a-Si modules under sunlight exposure. (b) Data of *Isc* at Standard Test Conditions (STC) during the stabilization process. Stabilization is reached after two months.

Table 4
Manufacturer datasheet of the c-Si sensor used in 2012 tests. (STC * 1 sun (=100 mW/cm^2), air mass 1.5, 25 °C).

Parameter	Symbol	Test conditions	Results	Units
Open circuit voltage	Voc	STC*	0.63	V
Short circuit current	*Isc*	STC*	50	mA
Maximum power	Pm	STC*	22.3 (Vmp = 0.5 V; Imp = 44.6 mA)	mW

(d) The last part of the analysis consisted of a comparison of the normalized difference (ratio) between data averages at high and low positions for every day of the analysis. The objective of this step was to compare the stability of the differences between high and low measurements.

In the case of the first year, a set of comparative graphs were included to show how sunny and cloudy days affected irradiation at different positions inside the trees.

4. Results and discussion

4.1. Analysis of data captured using a-Si mini-modules

On sunny days, the irradiance is formed by three main components (direct irradiance, indirect irradiance or albedo (Enriquez et al., 2012), and diffuse irradiance (Li et al., 2012). On the contrary, when the day is cloudy, the irradiance is mainly formed by diffused irradiance, and does not influence the different levels inside the canopy of the tree in the same manner. In general, for cells placed in an horizontal position inside the canopy, the albedo or ground reflection does not introduce any special contribution to the output signal but the light scattered from all the surrounding points (tree branches, leaves, etc.) could produce a similar effect. Also, the irradiance components change along the day (Padovan and Del Col, 2010).

In the dispersion graph of Fig. 4 it can be observed how the cumulated radiation of the different days was not quite stable throughout the days. There were only two days where the daily irradiation did not reach 15 MJ/m^2 in the horizontal plane over the trees. According to the data, the irradiation inside the trees was much lower than the global irradiation over the trees without shade. The irradiations during the period were usually lower than 8 MJ/m^2 at higher positions and bellow 4 MJ/m^2 at lower positions.

These irradiation data were unexpectedly low. The obtained results were affected by partial shadowing that impacted the measurement of the actual irradiation inside the tree. Notice that, in general, a partial shadow on a photovoltaic device introduces decay in its short circuit proportional to the shadowed area (e.g. a 20% shadowing could result in a 20% lower current). However, in the case of series-connected cells, the same partial shadow in the whole surface could affect a particular device on the series in its entirety. This cell would then limit the output of the mini-module (e.g. a 20% shadowing in the mini-module would result in a 80% lower current for a particular cell and therefore, a 80% lower current for the entire mini-module).The effect of a partial shadow in a particular cell would be equivalent to having all the cells in the module affected with the same amount of shadow (the results are the same if one, two or three cells became shadowed at the same time in terms of short-circuit current).

According to Fig. 5, the mean value for the irradiation received by the trees was always bellow 7 MJ/m^2 at both tested positions of the sensors (1.5 m and 3 m). The irradiation was expected to be lower inside the canopy than over the trees. Nevertheless, the results obtained were lower than expected. The partial shadows effect, more than likely affected the measured data and this was the reason for the lower measurements. However, this effect appears in both positions (high and low) so the most important result is

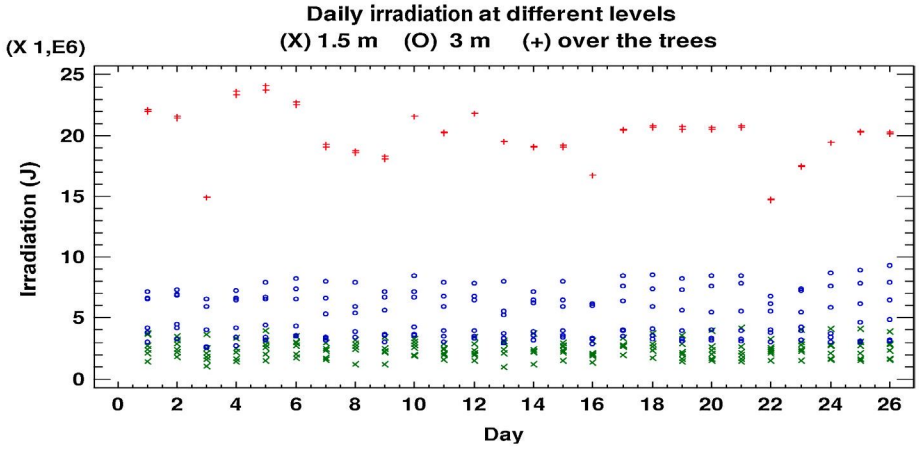

Fig. 4. Descriptive analysis using dot plot for daily irradiation at two levels of the six tested trees in 2011 test.

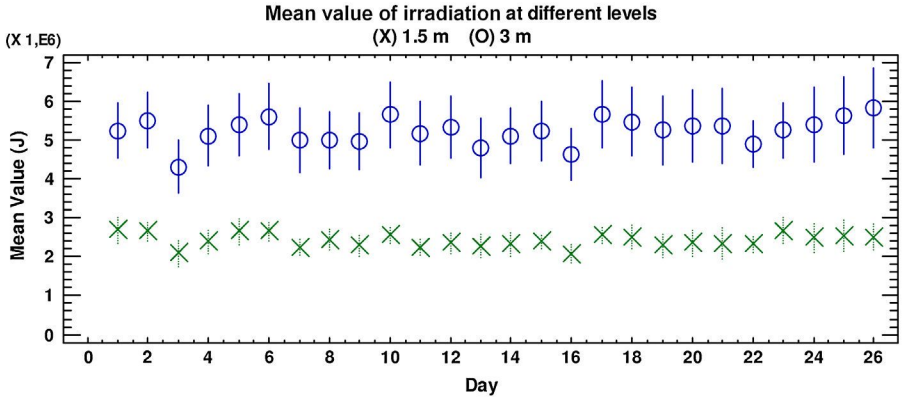

Fig. 5. Descriptive analysis of mean irradiation at different levels inside the tree for the different days in 2011 test.

the difference between the means of the measurements at difference levels. These results cannot be considered as quantitative but qualitative. The daily mean value for the irradiation at lower positions was around 2.5 MJ/m^2 which was less than half of the irradiation at higher positions, where the irradiation was around 6 MJ/m^2. It must be pointed out that the used days were mainly sunny and led to stable measurements.

The box and whisker analysis is presented in Fig. 6. The mean values and two main quartiles of the measurements of the sensors at high and low positions do not overlap in most of the trees. According to the data the measured irradiation was around 5 MJ/m^2 at high positions and 2.5 MJ/m^2 at low positions. The irradiation was around 50% lower at lower positions. It must be pointed out that such results only offer a qualitative measurement and not a precise quantitative measurement of the irradiation. Despite the problem with this type of sensor, the partial shadowing affects sensors situated in both positions: high and low. For this reason, the analysis is a viable method for determining the qualitative differences at different positions, but not the quantitative values of the solar irradiation.

Finally, in Fig. 7 we used a box and whisker graph to analyze the difference of the irradiation between high (3 m) and low (1.5 m) positions throughout the days. The

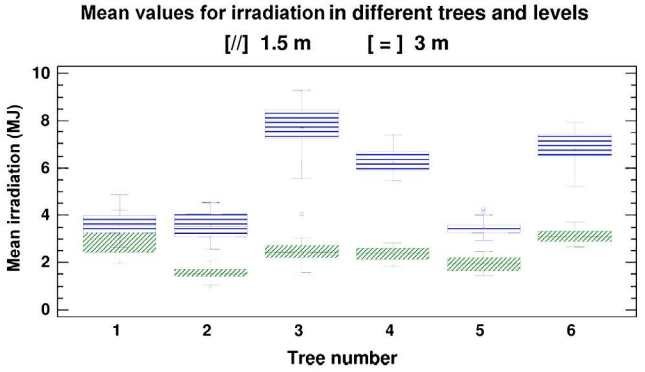

Fig. 6. Descriptive analysis using box and whisker for comparison of mean values of irradiation at 1.5 m and 3 m for the different trees in 2011 test.

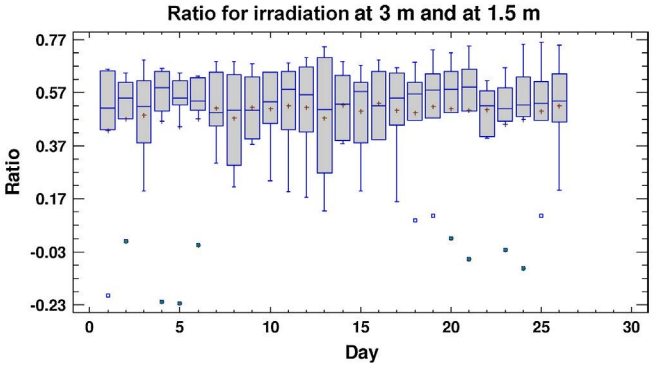

Fig. 7. Descriptive analysis of the difference between irradiation at 3 m and 1.5 m for the different days in 2011 test.

data is the normalized difference of the data at high and at low positions (ratio), that is, the difference of the data divided by the data at high position. It can be observed how the mean value of such a difference does not depend on the irradiation. The mean value is 49.3% ± 1.09% for a 95% confidence interval.

4.2. Analysis of data from c-Si cells

The second experiment was performed in September and October of 2012. The days were mainly cloudy and rainy and the data was not as homogeneous as in the previous year. In Fig. 8 it can be observed how the irradiation at the higher level had not increased significantly and hardly reached 20 MJ/m^2. In the same Fig., the data from a 3 m sensor of a tree (number 3) is even higher than data from reference cells in 15 cases. Depending on the position of the sensors and the leaves over it, it was possible that a sensor situated at a higher position received less radiation. This is why the important value is the mean value of all the sensors.

According to the data shown in Fig. 9 the values obtained from sensors at different levels are also different. In this experiment (2012) the irradiation measured was higher, reaching 12 MJ/m^2/day, than in the previous year

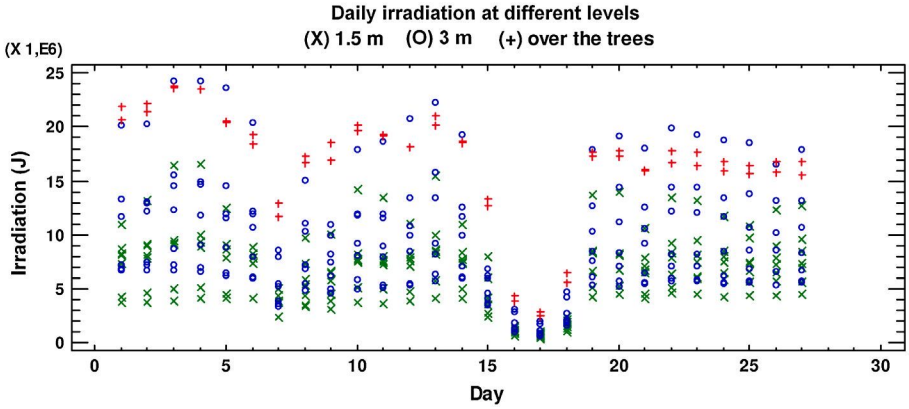

Fig. 8. Descriptive analysis using dot plot for daily irradiation at two levels of the seven tested trees in 2012 test.

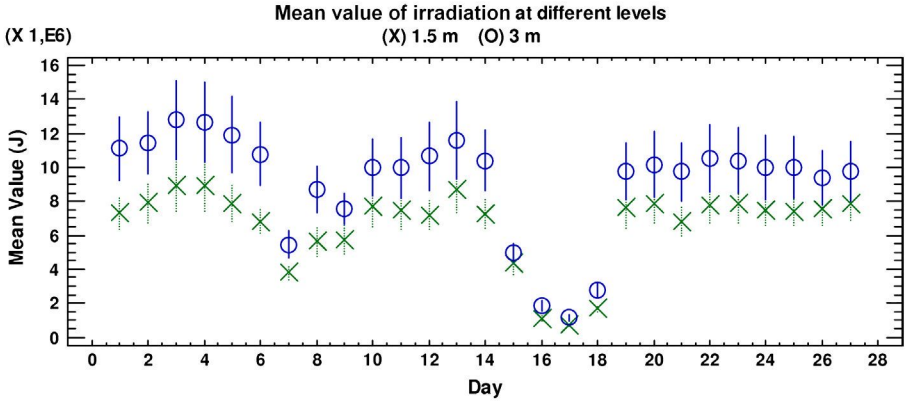

Fig. 9. Descriptive analysis of mean irradiation at different levels inside the tree for the different days in 2012 test.

(2011), where the maximum was 5 MJ/m^2/day. This result confirms that these sensors do not present the effect of partial shadowing that affected the real measurement in the 2011 experiment.

Also it can be observed that the relative differences are not so high than in the previous year. In 2012, the difference is nearly 25%, and in the year 2011 the difference was around 50%.

The analysis of the mean values at different levels in each tree can be observed in Fig. 10. The mean difference between 1.5 m and 3 m measurements was around 25%, which is not as big as in the experiment in 2011, where it was around 50%. Nevertheless, the irradiation levels are much higher at every position, even though this year the irradiation was lower. The reason is the absence of the partial shadows effect. As a result, the current that the cell provided was directly related to the level of the irradiance.

Pruning the branches of these trees to allow the sunlight to reach the lower parts of the trees may have affected the irradiation at lower positions, decreasing the difference

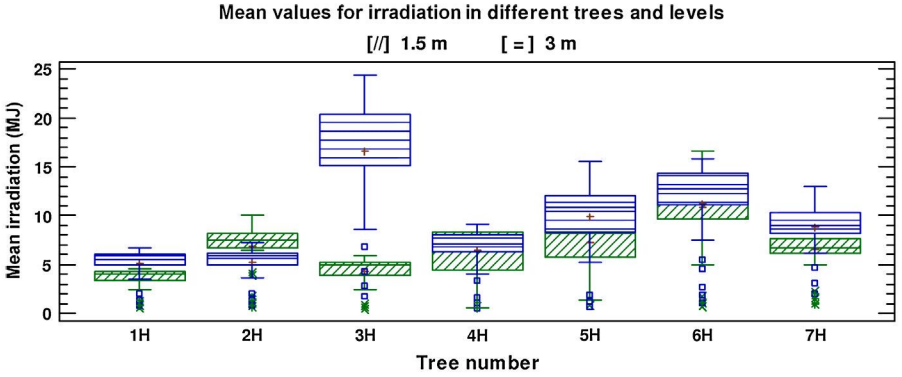

Fig. 10. Descriptive analysis using box and whisker for comparison of mean values of irradiation at 1.5 m and 3 m for the different trees in 2012 test.

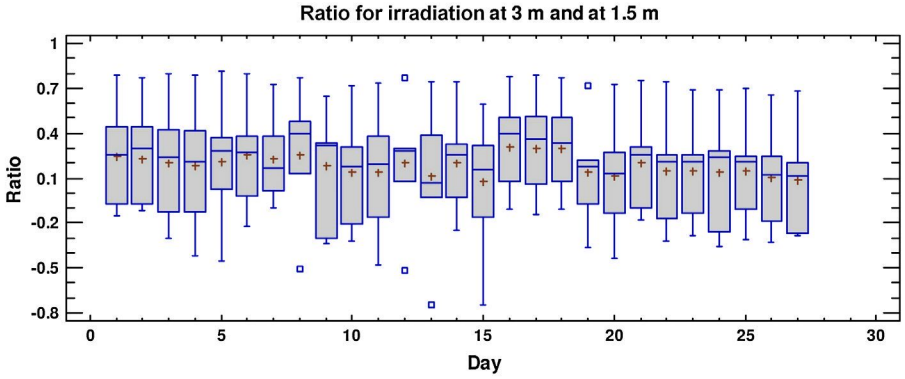

Fig. 11. Descriptive analysis of the difference between irradiation at 3 m and 1.5 m for the different days in 2012 test.

between the irradiation at higher and lower positions. Apart from the last consideration, the movement of the branches and the sensors, the wind must also be taken into account. The wind also influenced the fruits and was not considered as a problem but an inevitable situation.

As we did for the year 2011 (Fig. 11), we used a box and whisker graph to analyse the difference of the irradiation between high (3 m) and low (1.5 m) positions during the days in 2012. The influence of global irradiation must be considered. During the used period of 2012, the weather was not as stable compared to the 2011. There were many cloudy days and as a consequence, the variability was higher. The mean value for the mentioned difference was 18.5%±2.58% for a 95% confidence interval.

For the experiment in 2012, an analysis of variance (ANOVA) was performed in order to determine the relationship between position and solar irradiation received. As a conclusion, solar radiation penetration inside the canopy in 2012 shows a significant effect ($F = 60.9$, significant at level 0.01) on the top or bottom position and on the tree ($F = 31.9$, significant at level 0.01) (Gueymard, 2004).

5. Conclusions

Solar irradiation inside a tree canopy can be assessed using low-cost solar cell-based radiation sensors. Two kinds of sensors, a-Si series-connected mini-modules and single c-Si cells, were tested in two different measurement years.

According to the results, the use of mini-modules is only recommended when a qualitative and comparative analysis is going to be performed, as the quantitative error is high. Such error was around 50% due to the named "partial shadows" effect, where the shadowing of a cell of the mini-module affects the output current of the whole module.

On the other hand, the use of small c-Si cells based sensors is recommended for both qualitative and quantitative analysis of the irradiation received at different levels inside a tree canopy. In order to get more accurate results, it would be advisable to reserve one or two measuring channels in the DAQ systems to measure the working temperature of representative cells within the set of cells. This would allow the use of an effective temperature coefficient for the cell current and a more precise evaluation of the error introduced.

The irradiation is significantly higher at high positions (3 m) of apple trees, compared to low positions (1.5 m). Such irradiation reached 13 MJ/m^2 a day at higher positions and was around 20% (18.5% ± 2.58% for 95% of confidence interval) at lower positions.

The use of a data acquisition system based on a notebook computer does not pose advantages over a data logger based one. The energy consumption of the notebook computer was around 30 times higher than that of the data logger. This leads to a more complicated setup. Also, a computer is not reliable enough for work in temperature conditions with high variations during the day and night.

Acknowledgements

We would like to thank to VIRCOOP for the orchard supply, Álvaro Blanco and Jesús Val (Estación Experimental de AulaDei (CSIC)) for their help on the design of the experiment, Antonio Rabasco for his help on the field work and the EU project InsideFood (FP7-226783) for its financial support. The opinions expressed in this document do by no means reflect their official opinion or that of its representatives.

References

American Society for Testing and Materials ASTM Standard E490-00a(2006). Standard solar constant and zero air mass solar spectral irradiance tables, ASTM International, West Conshohocken, PA. doi: http://dx.doi.org/10.1520/E0490-00AR06, <http://www.astm.org>.

International Electrotechnical Commission, tul=0?>IEC 60904-3. Standard IEC 60904-3: photovoltaic devices. Part 3: Measurement principles for terrestrial photovoltaic (PV) solar devices with reference spectral irradiance data. IEC Central Office, Geneva, Switzerland.

Parisi, A.V., Kimlin, M.G., Wong, J.C.F., Wilson, M., 2000. Diffuse component of solar ultraviolet radiation in tree shade. J. Photochem. Photobiol., B 54, 116–120.

Zarzalejo, L., Polo, J., Martín, L., Ramírez, L., Espinar, B., 2009. A new statistical approach for deriving global solar radiation from satellite images. Sol. Energy 83 (4), 480–484.

Bois, B., Pieri, P., Van Leeuwen, C., Wald, L., Huard, F., Gaudillere, J.-P., Saur, E., 2008. Using remotely sensed solar radiation data for reference evapotranspiration estimation at a daily time step. Agric. For. Meteorol. 148, 619–630.

Geraldo-Ferreira, A., Soria-Olivas, E., Gómez-Sanchis, J., Serrano-López, A.J., Velázquez-Blazquez, A., López-Baeza, E., 2011. Modelling net radiation at surface using "in situ" netpyrradiometer measurements with artificial neural networks. Expert Syst. Appl. 38, 14190–14195.

Eltbaakh, Yousef, A., Ruslan, M.H., Alghoul, M.A., Othman, M.Y., Sopian, K., Fadhel, M.I., 2011. Measurement of total and spectral solar irradiance: overview of existing research. Renew. Sustain. Energy Rev. 15, 1403–1426.

Plesz, B., Földváry, Á., Bándy, E., 2011. Low cost solar irradiation sensor and its thermal behaviour. Microelectron. J. 42, 594–600.

Martin, N., Ruiz, J.M., 2001. Calculation of the PV modules angular losses under field conditions by means of an analytical model. Sol. Energy Mater. Sol. Cells 70 (1), 25–38.

Melado-Herreros, A., Muñoz-García, M.A., Blanco, A., Val, J., Fernandez-Valle, M., Barreiro, P., 2012. Relationship between solar radiation on watercore on apple fruit assessed with MRI. In: International Conference of Agricultural Engineering, CIGR-AgEng2012. Papers Book.

Pieri, Phillipe, 2010. Modelling radiative balance in a row-crop canopy: row-soil surface net radiation partition. Ecol. Model. 221, 791–801.

Palva, L., Markkanen, T., Siivola, E., Garam, E., Linnavuo, M., Nevasd, S., Manoochehri, F., Palmroth, S., Rajala, K., Ruotoistenmäki, H., Vuorivirta, T., Sépala, I., Vesala, T., Hari, P., Sepponen, R., 2001. Tree scale distributed multipoint measuring system of photosynthetically active radiation. Agric. For. Meteorol. 106, 71–80.

Abraha, M.G., Savage, M.J., 2010. Validation of a three-dimensional solar radiation interception model for tree crops. Agric. Ecosyst. Environ. 139, 636–652.

Heisler, G.M., Grant, R.H., Gao, W., 2003. Individual- and scattered-tree influences on ultraviolet irradiance. Agric. For. Meteorol. 120, 113–126.

Mariscal, M.J., Orgaz, F., Villalobos, F.J., 2000. Modelling and measurement of radiation interception by olive canopie. Agric. For. Meteorol. 100, 183–197.

LI-CORE, LI-189. <ftp://ftp.licor.com/perm/env/LI-189/Manual/LI-189%20Manual.pdf>.

International Electrotechnical Commission. Standard IEC 60891 ed2.0., 2009, Photovoltaic devices – procedures for temperature and irradiance corrections to measured I–V characteristics, IEC Central Office, Geneva, Switzerland. 1987.

Gueymard, C., 2004. The sun's total and spectral irradiance for solar energy applications and solar radiation models. Sol. Energy 76, 423–453.

Balenzategui, J.L., Chenlo, F., 2005. Measurement and analysis of angular response of bare and encapsulated silicon solar cells. Sol. Energy Mater. Sol. Cells 86, 53–83.

Melado-Herreros, A., Muñoz-García, M.A., Blanco, A., Val, J., Fernández-Valle, M.E., Pilar Barreiro, P., 2013. Assessment of watercore development in apples with MRI: effect of fruit location in the canopy. Postharvest Biol. Technol. 86, 125–133.

Enriquez, R., Zarzalejo, L., Jiménez, M.J., Heras, M.R., 2012. Ground reflectance estimation by means of horizontal and vertical radiation measurements. Sol. Energy 86 (11), 3216–3226.

Li, Huashan, Xianbiao, Bu, Long, Zhen, Zhao, Liang, Ma, Weibin, 2012. Calculating the diffuse solar radiation in regions without solar radiation measurements. Energy 44 (1), 611–615.

Padovan, A., Del Col, D., 2010. Measurement and modeling of solar irradiance components on horizontal and tilted planes. Sol. Energy 84 (12), 2068–2084.